Appendix

Phosphate immobilisation dynamics and interaction with arsenic sorption at redox transition zones in floodplain aquifers: Insights from the Red River Delta, Vietnam

Author list: Harald Neidhardt[1]*, Sebastian Rudischer[1], Elisabeth Eiche[2], Magnus Schneider[2], Emiliano Stopelli[3], Vu T. Duyen[4], Pham T.K. Trang[4], Pham H. Viet[4], Thomas Neumann[5], and Michael Berg[2]

and the AdvectAs team

[1]Geoecology, Eberhard Karls University Tübingen, 72070 Tübingen, Germany

[2]Institute of Applied Geosciences, Karlsruhe Institute of Technology, 76131 Karlsruhe, Germany

[3]Eawag, Swiss Federal Institute of Aquatic Science and Technology, 8600 Dübendorf, Switzerland

[4]Key Laboratory of Analytical Technology for Environmental Quality and Food Safety Control (KLATEFOS), VNU University of Science, Vietnam National University, Hanoi, Vietnam

[5]Applied Geochemistry, Technical University of Berlin, 10623 Berlin, Germany

AdvectAs team: Agnes Kontny, Alex Lightfoot, Andreas Kappler, Bhasker Rathi, Henning Prommer, Olaf Cirpka, Martyna Głodowska, Lenny H.E. Winkel, Monique Patzner, Rolf Kipfer, and Sara Kleindienst

*harald.neidhardt@uni-tuebingen.de

Table of contents:

Note A.1: Sediment core description

A detailed illustration of the sediment core including lithology, colour and total element concentrations is provided in Fig. 2 (main text). The top clayey silt layer had an overall thickness of 19 m and was characterised by a very heterogenous stratigraphy. The section between 3 and 11.5 m bls comprised several thin layers of dark brown, grey and black coloured sediments, often exhibiting large quantities of organic matter. Below, bleached grey sediments followed between 11.5 and 15.5 m bls. The remaining clayey silt deposits (15.5 to 19 m bls) consisted mainly of orange coloured sediments, but also included two thin grey layers at 18.2 and 18.5m bls. The grain size in the first 19 m was dominated by the clay and silt fraction, with thin layers of intercalated sandy silt deposits at 3, 8 and 15 m bls.

At 19 m bls, the transition to the aquifer was marked by orange loamy and sandy sediments, indicating moderately reduced redox properties. At 20.5 m bls, the first redox transition was met and the sediment colour changed from yellow-orange to grey. The grey sands extended to a depth of 30 m bls and were only intersected sparsely by a small fingers of orange sand of few centimetres thickness at 22.5 m bls. Between 29.5 and 30.5m bls the colour of the aquifer sands changed again to yellow-orange colours, indicating less reducing redox properties of the deposits to a depth of 41m bls. Several small bands of grey sediments occurred at 34.4 and 37.5 m bls. The last major redox change was located at a depth of 41 m bls as indicated by multiple alternating layers of orange (moderately reduced) and grey (strongly reduced) coloured sediments. The sediments of the aquifer were generally dominated by fine to coarse sand, only between 32 and 36 m bls several small clayey silt intrusions of only few centimetres thickness occurred. Redox properties ranged from moderately reduced (as indicated by orange and yellow-orange colour) to highly reduced (reflected by grey colour), but also included thin sections of mixed redox properties (see Fig. 1, main text). In summary, the sand aquifer can be subdivided into a predominantly grey upper part (20.5-29.5 m) and a more orange to yellow-orange lower part (29.5-41 m). Redox interfaces with strong colour contrasts reflecting redox gradients are visible throughout the aquifer sediments, especially at lithological boundaries.

Between 43 and 46.5 m bls, a clayey silt layer representing an aquitard was met, which covered a gravel layer (note: no samples could be recovered from the gravel layer).

Note A.2: Evaluation of the sequential extraction procedure

In this note, several approaches are presented that were used to ensure that the analytical results of the optimised sequential extraction procedure are reliable, and that the extraction solutions are interpreted correctly for the phosphorus (P) and arsenic (As) pool composition of the analysed samples.

Quality controls, ICP-OES analysis: To generally ensure the reliability of the ICP-OES analysis (sequential extraction solutions and acid pressure digestions), certified reference materials were included as quality controls (Multi Element ICP Standard Solution and Single Element Standards for As and P, all Carl Roth GmbH). Recovery rates for P, As, Al, Fe, Ca, Mg, and Mn of the quality controls ranged between 95% to 112%, with a precision of ± 5% relative standard deviation (RSD) for replicate analyses. Blank solutions were included in all extraction runs to check the chemicals used, which indicated no impurities or other contaminations.

Quality controls, sequential extraction: The certified P reference material River Sediment (BCR®-684, Institute for Reference Materials and Measurements) was extracted (n=1) with the sequential extraction scheme. The sum of extractable P concentrations in all extractions agreed well with the certified concentrations for total PO_4^{3-}, P_{org}, and P_{tot}, with recovery rates of 97.4, 92.3, and 92.9%, respectively. For As, the reference material Metals in Soil (SQC001-30G, lot LRAC3749, Sigma Aldrich) was extracted (n=1). Here. the sum of extractable As compared to the certified As_{tot} concentration yielded a recovery rate of 114%.

Carry-over effects: Sequential extraction procedures are known to be susceptible to carry-over effects (Hupfer *et al.*, 2009). Due to the removal of weakly and strongly surface sorbed PO_4^{3-}, P_{org}, and As by the $NaHCO_3$- and NaOH-extraction solutions, re-adsorption may occur during the extraction, which would result in a carry-over into the following extraction pools (Baldwin, 1996). The required number of repetitions was tested with PO_4^{3-} for a separate sample set comprising clayey silt as well as orange (i.e. moderately reduced) and grey (i.e. highly reduced) aquifer sand (Fig. A.1). Based on the outcomes, three repetitions were included for the $NaHCO_3$ and the NaOH extractions, each with a duration of 30 minutes (Table 1, main text). Also, three additional $NaHCO_3$ extraction steps (each for 30 minutes) were included in the CDB extraction to avoid re-adsorption of released PO_4^{3-}, P_{org}, and As to free sorption sites. Finally, a step with Milli-Q water was included at the end of each step to

neutralise the pH values in between the extractions (Table 1, main text). The shaking time for repetitions and washes was reduced to 30 minutes.

To ensure that all extracted P and As was removed from the samples, three 30 minutes extractions with Milli-Q water were included for the HCl and H_2SO_4 extractions. Here, Milli-Q was preferred over $NaHCO_3$ to avoid a pronounced pH shift.

In presence of large amounts of Ca, secondary Ca-PO_4^{3-} minerals may form in alkaline extraction solutions (i.e. by the $NaHCO_3$, NaOH, and CDB extracts) as highlighted by Hupfer et al. (Hupfer *et al.*, 2009), which would result in a carry-over of PO_4^{3-} into the HCl pool. However, this possibility was ruled out by carrying out a PO_4^{3-} standard addition test for the $NaHCO_3$ extraction (pH 8.5). Three representative samples with comparatively high Ca concentrations (two clayey silt samples with 3.19 and 1.10 g kg^{-1}, and one grey sand sample with 0.33 g kg^{-1}) were selected and extracted in parallel adding additional PO_4^{3-}, in three different concentrations (+0, +588 and +1176 µg L^{-1} PO_4-P). The results indicated no formation of secondary Ca-PO_4^{3-} minerals (i.e. full recovery of added PO_4^{3-}, see Fig. A.2). Generally, Ca_{tot} concentrations in the samples were low (ranging from 0.13 to 8.44 g kg^{-1}), and no $CaCO_3$ could be detected by reaction with 10% HCl. Furthermore, the average HCl-extractable Ca concentration was 1.45 g kg^{-1} for the clayey silt samples, 0.10 g kg^{-1} for the orange aquifer sand, and values below the detection limit for the reduced and mixed redox state sands (Table A.2).

To generally avoid alteration of the mineralogy by oxidation (the sediments were permanently in contact with anoxic groundwater before the samples were recovered in the field), all extraction solutions were deoxygenated before use and precautions were taken to minimise oxidation during sample handling and storage (further details provided in the materials and methods section of the main text).

Plausibility checks: In the following, further evaluation approaches are presented, which mostly refer to concentrations after conversion from mg L^{-1} into mg kg^{-1}.

The comparison of P_{tot} concentrations determined by acid pressure digestions with the sum of extractable P provides the possibility to calculate recovery rates. Here, the sum of extractable PO_4^{3-} (for the $NaHCO_3$ and CDB extraction solutions) and P_{tot} (for NaOH, HCl, and H_2SO_4 extracts) in the individual samples was highly correlated with the P_{tot} concentrations determined by acid pressure digestion, reaching an average recovery rate of 97.6 ± 25.4% (n=58, see Fig. A.3).

Note that extractable PO_4^{3-} concentrations were preferred over P_{tot} concentrations for the $NaHCO_3$ and CDB extracts because (i) all P was present as PO_4^{3-}, and (ii) the measurements by CFA were more

accurate as the ICP-OES, because the later required a dilution of the sample extracts that further lowered the generally low P concentrations.

For As, the average recovery rate of the samples was 61.7 ±17.5% (n=34, note: only aquifer sand samples were analysed by ICP-MS due to a limitation of measuring time and a high number of extraction solutions). The lower recovery rate for As was attributed to the presence of non-extractable As in stable minerals and the generally low As_{tot} concentrations ranging between 0.68 and 23.5 mg kg^{-1}.

For Ca, Fe, Mn, Al, the average recovery rates were 50.6 ± 37.2%, 86.0 ± 19.4%, 101 ± 50.4%, and 36.8 ± 8.3% (n=86), respectively. For Ca, concentrations in most extraction solutions were close to the methodological detection limit, resulting in a partial underdetermination. In the case of Al, the determination in the CDB extraction solution was problematic due to matrix interferences, resulting in large variations and an underdetermination of the Al concentration. Despite the underdetermination of Ca and Al, the distribution of these elements in the respective extraction solutions provides valuable information for the P pool composition as discussed in the following.

Reproducibility evaluation. To evaluate the reproducibility of the sequential extraction, an internal soil house standard was frequently included, which represents a $CaCO_3$-rich farmland soil that is routinely included in our laboratory analyses. Results for P measurements of the sequential extraction solutions (P_{tot} by ICP-OES and PO_4^{3-} by CFA and photometer) demonstrated a good reproducibility (RSD values between 6 and 19%, see Table A.3). Furthermore, the sum of extractable P was 691 mg kg^{-1} (RSD: 9%), yielding an average recovery rate of 105 ±9% (n=6) of the P_{tot} concentration that was determined by ICP-OES from acid pressure digestions.

For other elements, the reproducibility was also in a similar range as long as concentrations did not get close to the respective methodical detection limit. Only CDB-extractable Al showed a poor reproducibility due to matrix interferences (RSD: 55%).

Evaluation of the extraction solutions: Knowledge of the selectivity of the operationally defined sequential extractions pools is crucial for the interpretation. It was previously highlighted that the selectivity of extraction solutions can be limited depending on the sample properties (Hupfer *et al.*, 2009; Fedotov *et al.*, 2012). One possibility to validate a sequential extraction procedure is by using artificial samples with an exactly known composition of P and As pools and minerals (Klotzbücher *et al.*, 2019). However, the solubility of pure artificial mineral phases is usually different from natural mineral phases that occur in the environment, resulting in a limited comparability. We therefore

followed a different approach by evaluating the selectivity of the sequential extraction solutions based on the concentration of extracted main elements. Here, Ca, Fe, Mn, and Al concentrations were used as they represent key elements of potentially P- and As-containing mineral phases.

Calcium: As expected, the majority of Ca was HCl-extractable (Table A.2). Only some minor proportions of Ca were extractable by H_2SO_4 and CDB, but only for clayey silt samples. Hence, the dissolution of Ca-PO_4^{3-} and -As minerals was achieved as expected through the HCl extraction. The Ca extracted by H_2SO_4 likely originated from the partial dissolution of more recalcitrant Ca-containing minerals such as feldspars or clays. The source of CDB-extractable Ca in the clayey silt samples remained open; however, since the pH in the CDB solution was 7.4, a dissolution of Ca-PO_4^{3-} and -As minerals could be excluded. One possible explanation is the release of surface sorbed and structurally bound Ca from metal-(oxyhydr)oxides, which were largely dissolved by the CDB solution as discussed in the following section.

Iron: The amount of Fe extracted by $NaHCO_3$, NaOH, and H_2SO_4 was negligible as compared to the CDB- and HCl-extractable Fe concentrations (Table A.2). The small amount of Fe that was $NaHCO_3$- and NaOH-extractable was attributed to the desorption of surface sorbed Fe^{2+} rather than the dissolution of Fe(III)-(oxyhydr)oxides (Mai *et al.*, 2014). This agreed with the elevated Fe^{2+} concentrations in migrating groundwater, which exceeded 9 mg L^{-1} (Neidhardt *et al.*, 2018; Stopelli *et al.*, 2020).

The amount of extractable Fe was in a similar range for both the CDB (representing weakly crystalline Fe(III)-(oxyhydr)oxides) and the HCl extracts (comprising crystalline Fe(III)(oxyhydr)oxides as well as Fe(II)- and mixed valence Fe(II,III)-minerals). Highest CDB-extractable Fe concentrations were associated with clayey silt and the orange aquifer sand (average concentration of 12.6 and 9.80 g kg^{-1}, respectively), while the lowest average concentration occurred in the reduced aquifer sand (3.33 g kg^{-1}). The concentration of HCl-extractable Fe was highest in the clayey silt samples (average of 13.9 mg kg^{-1}), and similar for the three aquifer sand classes (5.12 to 5.95 g kg^{-1}).

Manganese: For Mn, the pattern was highly similar to Fe, although average total and extractable Mn concentrations in the four sediment classes were generally one to two orders of magnitude lower (Mn_{tot} ranging from 131 to 641 mg kg^{-1}, Table A.2). The great majority of Mn was CDB- and HCl-extractable, while the Mn concentration was negligible (<11 mg kg^{-1}) for the other extracts. Similar to Fe, some Mn was NaOH-extractable, which is attributed to the desorption of surface sorbed Mn^{2+}.

Aluminium: The majority of Al was HCl- and CDB-extractable. However, some Al was already extracted by the NaOH solution (average concentration in clayey silt samples 3.38 g kg^{-1}, aquifer sands up to 0.73 g kg^{-1}) due to the increased solubility of Al-(oxyhydr)oxides under alkaline pH values (Klöppel *et al.*, 1997). Hence, the NaOH extraction did not only remove surface sorbed PO_4^{3-}, but also PO_4^{3-} and As that was structurally bound within Al-(oxyhydr)oxides (if present). As expected, Al was also largely released through the CDB extraction.

Concluding remarks: The following overview briefly summarises the key outcomes of the evaluation of the sequential extraction data.

- Extractions of certified standard materials showed a good accuracy for the certified values.
- Carry-over effects could be excluded as far as possible based on extraction repetition and standard addition tests.
- The plausibility check indicated excellent recovery rates for P, excluding a strong under- or overestimation of extractable P. For As, the extractable proportion was moderately underestimated as compared to the total concentrations.
- The sequential extraction results are reproducible as revealed by replicate analysis of an *in-house* standard.
- The elemental composition of the respective extraction solutions allowed us to evaluate which mineral phases and potential P and As pools were extracted, providing a solid foundation for the interpretation and discussion of the results. The detailed summary of targeted P and As pools and mobilisation mechanisms for each extractant is provided in Table 1 (main text).

In sum, the operationally defined extraction pools were limited to some extent regarding their selectivity, but we are confident that the obtained data provides valuable information for the sedimentary P and As pool composition at the redox transition zone. By comparing samples reflecting different redox properties, we are further convinced that we are able to draw reliable conclusions for the mechanisms underlying the immobilisation of dissolved PO_4^{3-} and interactions with As in the aquifer sediments that are influenced by long-term contact with reducing groundwater.

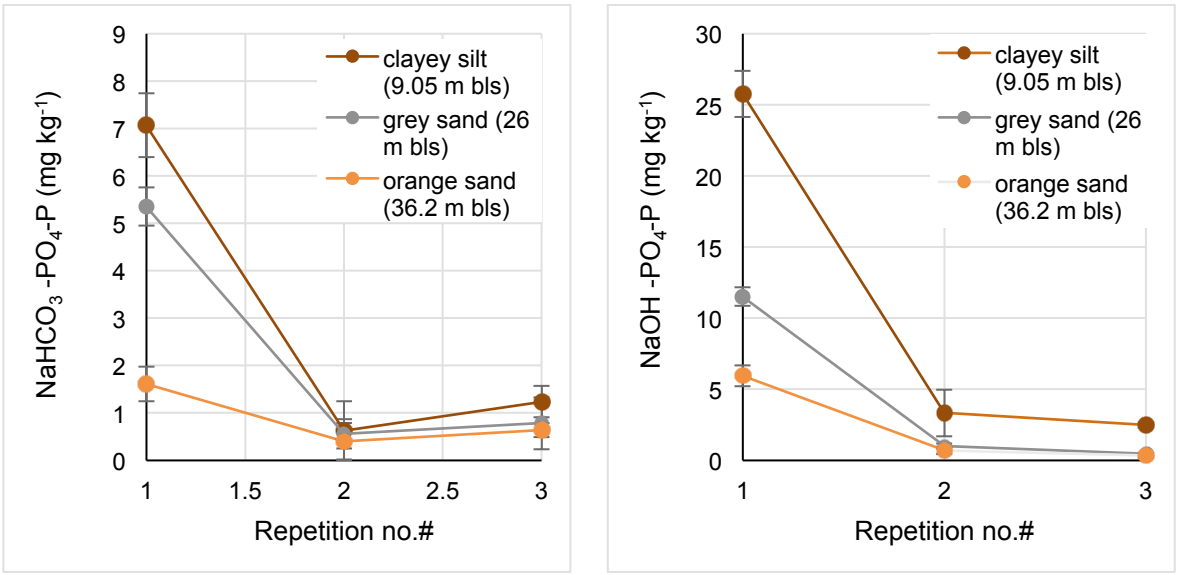

Fig. A.1. Determination of PO_4^{3-} in each individual repetition of the $NaHCO_3$ and NaOH extraction solutions. The number of repetitions was increased to three based on these outcomes.

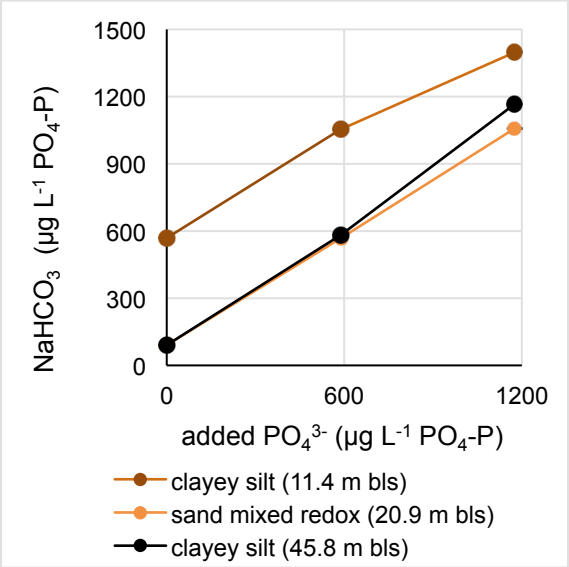

Fig. A.2. Standard addition test for three representative samples with comparatively high Ca_{tot} concentrations. Results indicate no loss of PO_4^{3-} due to the formation of Ca-PO_4^{3-} minerals during the extraction.

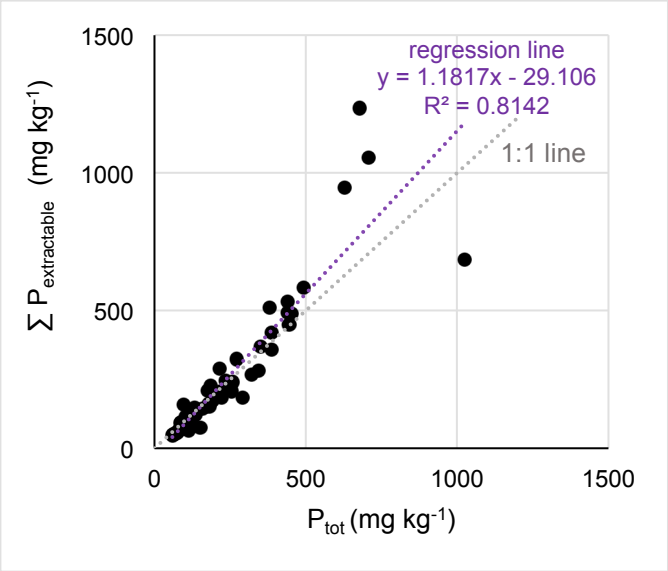

Fig. A.3. Scatterplot of P_{tot} obtained from acid pressure digestions and sum of extractable P ($\sum P_{extractable}$; as PO_4-P for the $NaHCO_3$ and CDB extraction solutions, and P_{tot} for the NaOH, HCl, and H_2SO_4 extraction solutions).

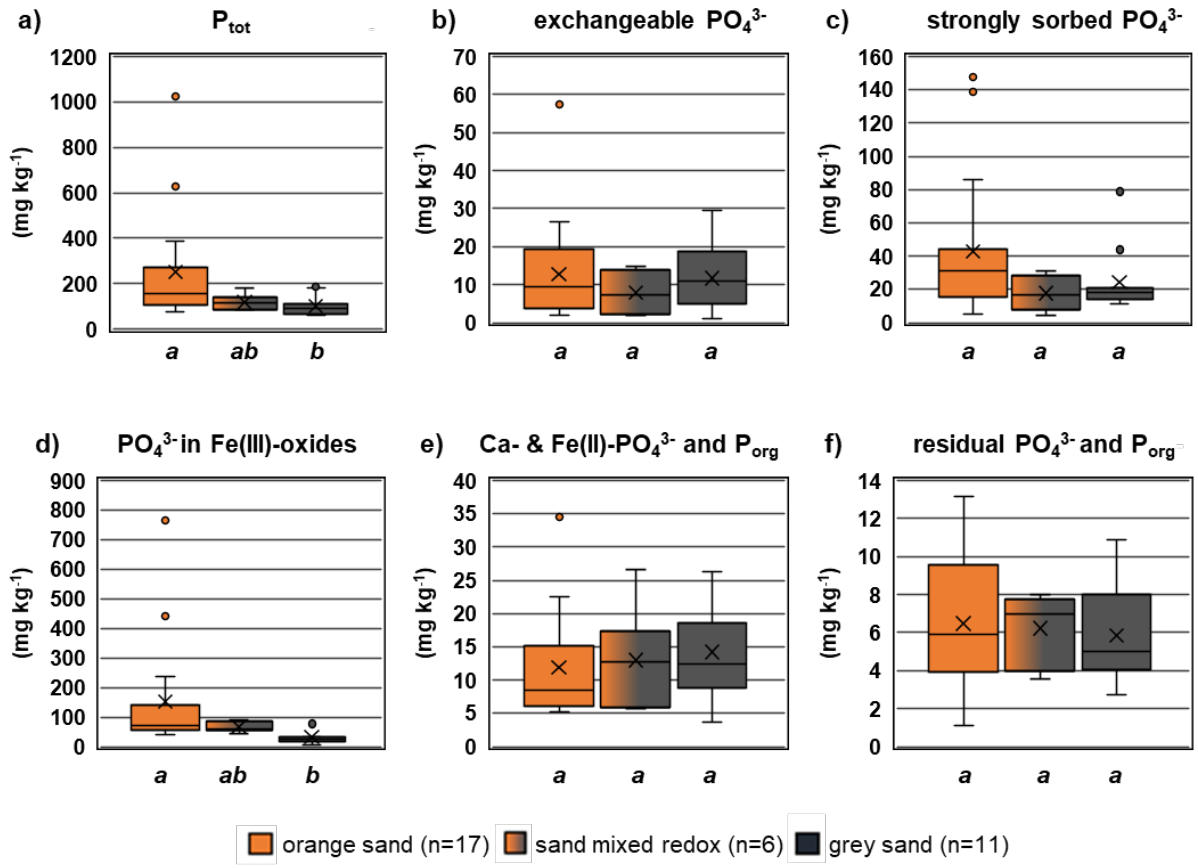

Fig. A.4. Boxplots illustrating the distribution of P_{tot} concentrations (a) and the concentration of extractable P (mg kg^{-1}) in the five sequential extraction pools (b-f) for the three different sediment classes. The P pools of the sediments were strongly linked to the redox state. Different lower-case letters (i.e. *a, b*) below the bars indicate significant differences between the respective aquifer sand classes (pair-wise post-hoc test, p <0.05).

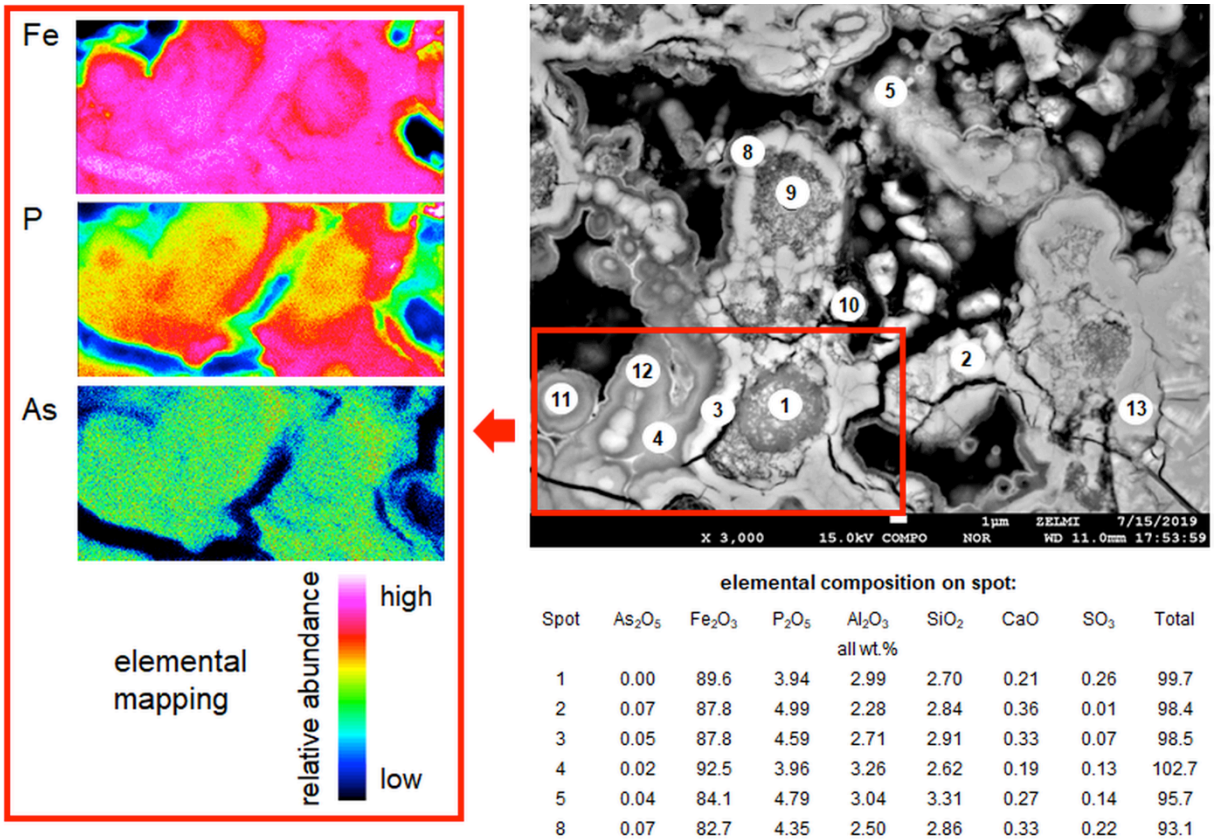

elemental composition on spot:

Spot	As_2O_5	Fe_2O_3	P_2O_5	Al_2O_3	SiO_2	CaO	SO_3	Total
				all wt.%				
1	0.00	89.6	3.94	2.99	2.70	0.21	0.26	99.7
2	0.07	87.8	4.99	2.28	2.84	0.36	0.01	98.4
3	0.05	87.8	4.59	2.71	2.91	0.33	0.07	98.5
4	0.02	92.5	3.96	3.26	2.62	0.19	0.13	102.7
5	0.04	84.1	4.79	3.04	3.31	0.27	0.14	95.7
8	0.07	82.7	4.35	2.50	2.86	0.33	0.22	93.1
9	0.05	83.4	4.01	2.47	2.76	0.21	0.08	93.0
10	0.02	92.5	3.71	2.57	3.20	0.33	0.07	102.4
11	0.03	87.4	4.00	3.47	2.75	0.22	0.35	98.2
12	0.05	83.1	3.77	2.90	2.38	0.18	0.79	93.2
13	0.06	87.8	4.99	2.49	3.04	0.46	0.02	98.9

Fig. A.5. Example of layered Fe(III)-(oxyhydr)oxide dominated cementations discovered in silty sand at the redox transition zone at 40 m bls. Such Fe(III)-(oxyhydr)oxide precipitates were detected at 20-22, 30, and 40 m bls, where aquifer sands increased were characterised by an increased silt proportion and mixed redox properties. The sample originated from a parallel drilling core (RD42), which was obtained approx. 10 m next to the core presented in this paper. The elemental composition of 11 spots and for a larger region of interest (see red box) were mapped by Electron Probe Microanalysis (EPMA) including a wavelength dispersive x-ray fluorescence detector (WD-XRF, acceleration voltage: 15kV). The elemental composition on-spot is reported in weight percentage (wt.%, see spots no. 1-13). For the elemental mapping, relative abundances of Fe, P, and As are illustrated (see red box in down left corner). Note that P and As are structurally bound within the precipitate and are not restricted to the surface.

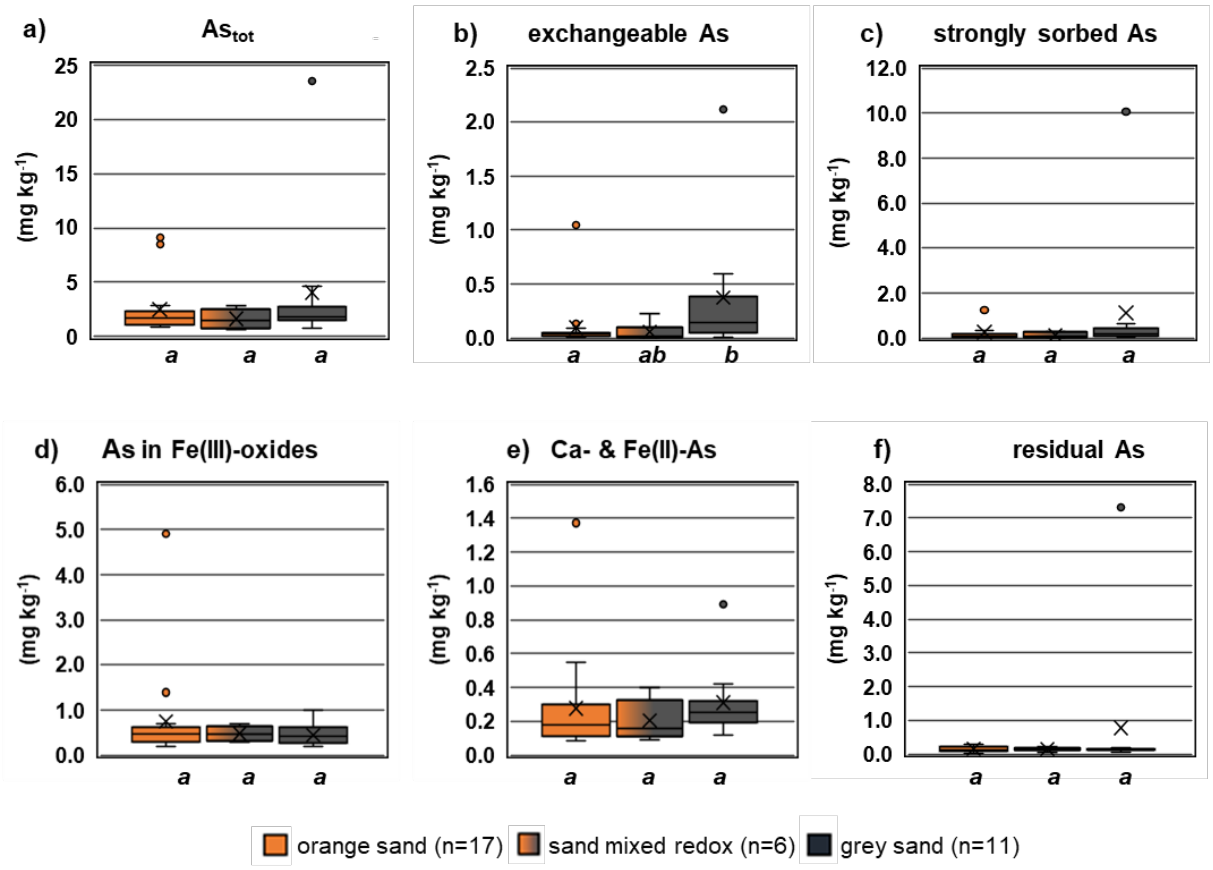

Fig. A.6. Boxplots illustrating the distribution of As_{tot} concentrations (a) and the concentration of extractable As (mg kg^{-1}) in the five sequential extraction pools (b-f) for the three different sediment classes. The P pools of the sediments were partially linked to the redox state. Different lower-case letters (i.e. *a, b*) below the bars indicate significant differences between the respective aquifer sand classes (pair-wise post-hoc test, p <0.05).

Table A.1. Overview of analytical details. Methodological detection limits (mdl) in mg kg^{-1} referring to sample targeted weights, calculated based on extraction blank solutions (3-times standard deviation of blank samples, n=7 for acid pressure digestions, and n=10 for the sequential extractions). For the ICP-MS analysis, background equivalent concentrations (BEC) based on the sample targeted weights are reported (in mg kg^{-1}), because extraction blanks were not analysed. For the Element Analyzer analyses, mdl values for C_{tot} and N_{tot} are reported in g kg^{-1} for a targeted sample weight of 0.4 g.

analysis:	Microwave assisted acid pressure digestions by ICP-OES (sample weight: 0.5 g):					
variable:	P_{tot}	Ca_{tot}	Fe_{tot}	Al_{tot}	Mn_{tot}	As_{tot}
details:	ICP-OES (213.617 nm axial)	ICP-OES (317.933 nm radial)	ICP-OES (238.204 nm axial)	ICP-OES (396.153 nm radial)	ICP-OES (257.610 nm radial)	ICP-OES (188.979 nm axial)
mdl (mg kg^{-1}):	0.92	56.1	7.65	22.6	4.23	0.28

analysis:	Sequential extraction solutions by ICP-OES and CFA (sample weight: 0.5 g):							
variable:	$NaHCO_3$-P	$NaHCO_3$-PO_4-P	NaOH-P	NaOH-PO_4-P	CDB-P	CDB-PO_4-P	HCl-P	H_2SO_4-P
details:	ICP-OES (213.617 nm axial)	UV-vis (660 nm)	ICP-OES (213.617 nm axial)	UV-vis (660 nm)	ICP-OES (213.617 nm axial)	CFA (880 nm)	ICP-OES (213.617 nm axial)	ICP-OES (213.617 nm axial)
mdl (mg kg^{-1}):	3.75	0.58	0.58	3.10	20.5	4.70	0.51	0.34

analysis:	Sequential extraction solutions by ICP-OES (sample weight: 0.5 g):							
variable:	NaOH-Fe	CDB-Fe	HCl-Fe	H_2SO_4-Fe	NaOH-Mn	CDB-Mn	HCl-Mn	H_2SO_4-Mn
details:	ICP-OES (238.204 nm axial)	ICP-OES (238.204 nm axial)	ICP-OES (238.204 nm axial)	ICP-OES (238.204 nm axial)	ICP-OES (257.610 nm radial)	ICP-OES (257.610 nm radial)	ICP-OES (257.610 nm radial)	ICP-OES (257.610 nm radial)
mdl (mg kg^{-1}):	0.04	54.4	5.00	0.03	0.01	1.96	0.01	0.01

analysis:	Sequential extraction solutions by ICP-OES (sample weight: 0.5 g):			
variable:	NaOH-Ca	CDB-Ca	HCl-Ca	H_2SO_4-Ca
details:	ICP-OES (317.933 nm radial)	ICP-OES (317.933 nm radial)	ICP-OES (317.933 nm radial)	ICP-OES (317.933 nm radial)
mdl (mg kg^{-1}):	2.44	150.48	0.32	0.16

analysis:	Sequential extraction solutions by ICP-MS (sample weight: 0.5 g):						
variable:	$NaHCO_3$-Fe	$NaHCO_3$-Mn	$NaHCO_3$-As	NaOH-As	CDB-As	HCl-As	H_2SO_4-As
details:	H_2 56	He 55	O_2 75-91	O_2 75-91	O_2 75-91	O_2 75-91	O_2 75-91
BEC (mg kg^{-1}):	0.80	0.25	0.01	0.01	0.10	0.02	0.01

analysis:	Element Analyzer (sample weight: 0.4 g)	
variable:	N_{tot}	C_{tot}
mdl (g kg^{-1}):	0.3	0.1

Table A.2. Overview of average total and extractable concentrations of Ca, Fe, Mn and Al. n.d. = not determined.

	Ca_{tot} (mg kg^{-1})	$NaHCO_3$-Ca (mg kg^{-1})	NaOH-Ca (mg kg^{-1})	CDB-Ca (mg kg^{-1})	HCl-Ca (mg kg^{-1})	H_2SO_4-Ca (mg kg^{-1})
clayey silt (n=24)	2790 ±2800	n.d.	<1.22	527 ±770	1450 ±2090	126 ±86
orange sand (n=17)	561 ±308	n.d.	<1.22	<75.2	104 ±227	28.7 ±38.7
grey sand (n=11)	500 ±347	n.d.	<1.22	<75.2	61.2 ±56.0	24.2 ±26.9
sand mixed redox (n=6)	566 ±216	n.d.	<1.22	<75.2	61.5 ±71.0	13.0 ±15.7

	Fe_{tot} (mg kg^{-1})	$NaHCO_3$-Fe (mg kg^{-1})	NaOH-Fe (mg kg^{-1})	CDB-Fe (mg kg^{-1})	HCl-Fe (mg kg^{-1})	H_2SO_4-Fe (mg kg^{-1})
clayey silt (n=24)	31100 ±20800	n.d.	825 ±842	12600 ±16600	13900 ±10600	941 ±417
orange sand (n=17)	18600 ±11700	6.72 ±11.1	61.3 ±73.6	9800 ±8770	5120 ±2000	324 ±138
grey sand (n=11)	11500 ±2390	4.79 ±1.60	105 ±116	3330 ±1280	5950 ±767	363 ±152
sand mixed redox (n=6)	12300 ±2850	2.85 ±1.08	99.2 ±172	5740 ±1250	5240 ±1410	333 ±44

	Mn_{tot} (mg kg^{-1})	$NaHCO_3$-Mn (mg kg^{-1})	NaOH-Mn (mg kg^{-1})	CDB-Mn (mg kg^{-1})	HCl-Mn (mg kg^{-1})	H_2SO_4-Mn (mg kg^{-1})
clayey silt (n=24)	436 ±426	n.d.	10.2 ±11.5	205 ±485	334 ±480	5.02 ±2.57
orange sand (n=17)	463 ±655	2.66 ±3.84	0.95 ±1.48	303 ±576	155 ±228	1.39 ±0.61
grey sand (n=11)	131 ±54	0.65 ±0.27	0.59 ±1.31	18.5 ±11.6	110 ±83	1.54 ±1.02
sand mixed redox (n=6)	641 ±618	2.35 ±1.54	1.76 ±2.42	568 ±608	198 ±146	1.29 ±0.33

	Al_{tot} (mg kg^{-1})	$NaHCO_3$-Al (mg kg^{-1})	NaOH-Al (mg kg^{-1})	CDB-Al (mg kg^{-1})	HCl-Al (mg kg^{-1})	H_2SO_4-Al (mg kg^{-1})
clayey silt (n=24)	48100 ±13500	n.d.	3380 ±3530	709 ±628	6150 ±2990	6220 ±1880
orange sand (n=17)	19400 ±8090	n.d.	730 ±760	653 ±528	2990 ±1340	2800 ±1330
grey sand (n=11)	18900 ±5140	n.d.	513 ±301	165 ±212	3290 ±651	2910 ±541
sand mixed redox (n=6)	16600 ±5690	n.d.	464 ±127	605 ±1041	3230 ±347	2740 ±558

Table A.3. Average element concentrations and relative standard deviation (%RSD) of the internal house standard (n=6). Total element concentrations determined by ICP-OES from acid pressure digestions and sequential extraction solutions, P in the $NaHCO_3$ and CDB extraction solution measured as PO_4^{3-} by photometer and CFA, respectively. Note that the internal house standard extractions were not analysed by ICP-MS, which is why no data is available for some elements and extraction solutions (listed as "n.d.", not determined).

variable:	acid pressure digestion	$NaHCO_3$	NaOH	CDB	HCl	H_2SO_4
P_{tot} (mg kg^{-1}; %RSD):	657 ±1%	23.5 ±19%	63.6 ±8%	144 ±12%	459 ±9%	33 ±10%
PO_4-P (mg kg^{-1}; %RSD):	n.d.	24.3 ±9%	23.8 ±6%	111 ±11%	n.d.	n.d.
As (mg kg^{-1}; %RSD):	10.5 ±3%	n.d.	n.d.	n.d.	n.d.	n.d.
Ca (mg kg^{-1}; %RSD):	80400 ±1%	n.d.	281 ±49%	5530 ±11%	90200 ±8%	132 ±32%
Fe (mg kg^{-1}; %RSD):	18800 ±1%	n.d.	756 ±5%	7030 ±10%	8880 ±7%	512 ±9%
Mn (mg kg^{-1}; %RSD):	538 ±1%	n.d.	8.58 ±9%	318 ±10%	243 ±8%	4.05 ±9%
Al (mg kg^{-1}; %RSD):	25400 ±6%	n.d.	1720 ±8%	1040 ±55%	5580 ±8%	1970 ±7%

Supplementary Information Literature

Baldwin, D. S. (1996). The phosphorus composition of a diverse series of Australian sediments. *Hydrobiologia*, **335**, 63-73.

Fedotov, P. S., Kördel W., Miró M., Peijnenburg W. J., Wennrich R., Huang P.-M. (2012). Extraction and fractionation methods for exposure assessment of trace metals, metalloids, and hazardous organic compounds in terrestrial environments. *Critical reviews in environmental science technology and Health Care*, **42**, 1117-1171.

Hupfer, M., Zak D., Roßberg R., Herzog C., Pöthig R. (2009). Evaluation of a well-established sequential phosphorus fractionation technique for use in calcite-rich lake sediments: identification and prevention of artifacts due to apatite formation. *Limnology and Oceanography: Methods*, **7**, 399-410.

Klöppel, H., Fliedner A., Kördel W. (1997). Behaviour and ecotoxicology of aluminium in soil and water-Review of the scientific literature. *Chemosphere*, **35**, 353-363.

Klotzbücher, A., Kaiser K., Klotzbücher T., Wolff M., Mikutta R. (2019). Testing mechanisms underlying the Hedley sequential phosphorus extraction of soils. *Journal of Plant Nutrition and Soil Science*, **182**, 570-577.

Mai, T. H., Postma D., Thi Kim Trang P., Jessen S., Hung Viet P., Larsen F. (2014). Adsorption and desorption of arsenic to aquifer sediment on the Red River floodplain at Nam Du, Vietnam. *Geochim Cosmochim Acta*, **142**, 587-600.

Neidhardt, H., Schoeckle D., Schleinitz A., Eiche E., Berner Z., Tram P. T. K., Lan V. M., Viet P. H., Biswas A., Majumder S., et al. (2018). Biogeochemical phosphorus cycling in groundwater ecosystems – Insights from South and Southeast Asian floodplain and delta aquifers. *Science of the Total Environment*, **644**, 1357-1370.

Stopelli, E., Duyen V. T., Mai T. T., Trang P. T. K., Viet P. H., Lightfoot A., Kipfer R., Schneider M., Eiche E., Kontny A., et al. (2020). Spatial and temporal evolution of groundwater arsenic contamination in the Red River delta, Vietnam: Interplay of mobilisation and retardation processes. *Science of the Total Environment*, **717**, 137143.